JGR Earth Surface

RESEARCH ARTICLE
10.1029/2023JF007324

Topography and Time Shape Mire Morphometry and Large-Scale Mire Distribution Patterns in the Northern Boreal Landscape

B. Ehnvall[1], J. L. Ratcliffe[1,2,3], M. B. Nilsson[1], M. G. Öquist[1], R. A. Sponseller[4], and T. Grabs[5]

[1]Department of Forest Ecology and Management, Swedish University of Agricultural Sciences, Umeå, Sweden, [2]North Highland College, Environmental Research Institute, University of the Highlands and Islands, Thurso, UK, [3]Unit for Field-Based Forest Research, Swedish University of Agricultural Sciences, Vindeln, Sweden, [4]Department of Ecology and Environmental Science, Umeå University, Umeå, Sweden, [5]Department of Earth Sciences, Geocentrum, Uppsala University, Uppsala, Sweden

Abstract Peatlands are major terrestrial soil carbon stores, and open mires in boreal landscapes hold a considerable fraction of the global peat carbon. Despite decades of study, large-scale spatiotemporal analyses of mire arrangement have been scarce, which has limited our ability to scale-up mire properties, such as carbon accumulation to the landscape level. Here, we use a land-uplift mire chronosequence in northern Sweden spanning 9,000 years to quantify controls on mire distribution patterns. Our objectives include assessing changes in the spatial arrangement of mires with land surface age, and understanding modifications by upland hydrotopography. Characterizing over 3,000 mires along a 30 km transect, we found that the time since land emergence from the sea was the dominant control over mire coverage, especially for the establishment of large mire complexes. Mires at the youngest end of the chronosequence were small with heterogenous morphometry (shape, slope, and catchment-to-mire areal ratios), while mires on the oldest surfaces were variable in size, but included larger mires with more complex shapes and smaller catchment-to-mire ratios. In general, complex topography fragmented mires by constraining the lateral expansion, resulting in a greater number of mires, but reduced total mire area regardless of landscape age. Mires in this study area occurred on slopes up to 4%, indicating a hydrological boundary to peatland expansion under local climatic conditions. The consistency in mire responses to spatiotemporal controls illustrates how temporal limitation in peat initiation and accumulation, and topographic constraints to mire expansion together have shaped present day mire distribution patterns.

Plain Language Summary Peatlands store nearly one third of the global soil carbon, despite covering only around three percent of the land surface. Open mires, which are characteristic peatland types at high latitudes, represent an important peat carbon store. Few studies have explored how mire patterns in the landscape change over time and space. This knowledge gap has limited our ability to estimate and scale-up mire properties, such as the peat carbon store, from the individual mire to the entire mire landscape. Here, we study the mire patch distribution in a landscape that covers nine thousand years of landscape development. Using this aging landscape, we can separate temporal controls on mire patterns from spatial controls related to local topography. We found that mire cover was mainly controlled by age, while the abundance of mires and their fragmentation was defined by local topography, for example, through the catchment-to-mire ratio and the slope of the surrounding upland areas, which define the limits for mire expansion upland. Our results provide an important step in understanding the spatial and temporal controls that give rise to present mire distribution patterns. Such information can further support landscape-level estimations of mire properties and functions, such as the long-term peat carbon store.

Key Points:

- Mire cover and shape are linked to the formation of large mire complexes, while abundance and fragmentation are driven by topography
- Areas of recent isostatic uplift hold small mires, while diverse initiation and expansion lead to heterogeneous mire patches in older areas
- Scaling up mire properties to the landscape level requires an understanding of spatiotemporal controls behind mire distribution patterns

Supporting Information:

Supporting Information may be found in the online version of this article.

Correspondence to:

B. Ehnvall and M. G. Öquist,
betty.ehnvall@slu.se;
mats.oquist@slu.se

Citation:

Ehnvall, B., Ratcliffe, J. L., Nilsson, M. B., Öquist, M. G., Sponseller, R. A., & Grabs, T. (2024). Topography and time shape mire morphometry and large-scale mire distribution patterns in the northern boreal landscape. *Journal of Geophysical Research: Earth Surface*, *129*, e2023JF007324. https://doi.org/10.1029/2023JF007324

Received 10 JUL 2023
Accepted 11 JAN 2024

Author Contributions:

Conceptualization: B. Ehnvall, J. L. Ratcliffe, M. B. Nilsson, M. G. Öquist, R. A. Sponseller, T. Grabs
Data curation: B. Ehnvall
Formal analysis: B. Ehnvall
Funding acquisition: M. B. Nilsson
Methodology: B. Ehnvall, M. B. Nilsson, T. Grabs
Project Administration: M. G. Öquist
Software: B. Ehnvall, T. Grabs

1. Introduction

Mires (fens and bogs) are peat-forming wetlands that, together with forests and lakes, create a landscape mosaic that is characteristic of much of the boreal biome. These ecosystems are critical for carbon sequestration (Loisel et al., 2014; Nilsson et al., 2008) and concomitant climate change mitigation (Frolking & Roulet, 2007). Mires also influence landscape biodiversity (Joosten, 2003) and regulate hydrological and biogeochemical processes of the wider catchment, including connections to forest and downstream water bodies (Ketcheson et al., 2016;

Supervision: M. B. Nilsson, M. G. Öquist, T. Grabs
Validation: J. L. Ratcliffe, T. Grabs
Visualization: B. Ehnvall
Writing – original draft: B. Ehnvall
Writing – review & editing: B. Ehnvall, J. L. Ratcliffe, M. B. Nilsson, M. G. Öquist, R. A. Sponseller, T. Grabs

Krachler et al., 2016; Sponseller et al., 2018). The types and magnitudes of ecosystem services provided by mires are strongly influenced by their spatial arrangement (Lane et al., 2018). For example, depending on their landscape position, mires can act as sinks, sources, or transformers of energy and matter to downstream water bodies (Fergus et al., 2017; Helbig et al., 2020a, 2020b; Lane et al., 2018). Nevertheless, little is known about how different drivers influence mire morphology and patterns at large-scales and how these controls may change over thousands of years of mire development at high latitudes.

Generally, the persistence of individual mires depends on a combination of classic soil formation factors, including climate, parent material and topography (Treat et al., 2019), but also on plant community composition and productivity (Kolari et al., 2021) and the degree of hydrological connectivity with the surrounding landscape (Fergus et al., 2017). The lateral expansion of mires may also be limited or favored by these same factors (Korhola, 1994; Loisel et al., 2013; Weckström et al., 2010). However, to understand drivers of mire morphometry and patterns at larger scales, it is necessary to consider these ecosystems as a part of the boreal landscape mosaic. Mires, forests and lakes are all temporally dynamic systems, which can transition from one to another through internal ecosystem development (i.e., succession). Such succession is often slow but constant, and gradually modifies ecosystems. In addition to this long-term succession, ecosystem transitions throughout the last interglacial period have often been episodic, non-linear events following abrupt climate changes (Gear & Huntley, 1991; Ireland & Booth, 2011; Scheffer et al., 2012). Examples of such events are lake infillings (i.e., terrestrialization) in which lakes transition to mires (Ireland et al., 2013), while mires in turn may be overgrown and forested as hydrological conditions change (Gałka et al., 2017; Gear & Huntley, 1991). If soil moisture further shifts toward drier conditions, boreal forests may become sparser or even reach tree-less states (Scheffer et al., 2012). The reverse can also happen if soil moisture conditions become wetter, resulting in paludification of forests to mires (Crawford et al., 2003; Novenko et al., 2018) or the formation of mire pools through aqualysis (Arlen-Pouliot & Payette, 2015). Thus, despite bi-stability between mires and forests under certain wetness conditions (Ohlson et al., 2001; Ratcliffe et al., 2017; Velde et al., 2021), local hydrologic conditions constitute a master control on the co-existence between these landscape elements (Ivanov, 1981).

In a landscape with a spatially homogenous climate and parent material, the hydrological conditions and soil wetness within and around mires are mainly defined by topography. From a local perspective, topography shapes mires by promoting greater lateral expansion rates in flat surroundings and by restricting this expansion in steeper areas such as local ridges (Almquist-Jacobson & Foster, 1995; Ehnvall, Ratcliffe, Bohlin, et al., 2023; Kulczyński, 1949; Rydin et al., 2013). At a regional scale, broader changes in topography also shape hydrological flowpaths (Graniero & Price, 1999), resulting in variable connections between upslope recharge areas and downslope discharge areas. Hence, the properties of hydrologically-connected upslope areas influence the biogeochemical characteristics of minerogenic mires (fens; Sjörs & Gunnarsson, 2002; White & Payette, 2016) as well as their functioning and resilience (Ivanov, 1981; Romanov, 1968). At the same time, the relative position of mires along a hydrological flowpath or stream determines its influence on downstream locations. In this way, topography plays an important role in redistributing biogeochemical elements vertically and horizontally across the landscape by mediating nutrient and sediment fluxes to and from mires (Ehnvall, Ågren, et al., 2023; Seibert et al., 2007).

Despite the wide-ranging significance of mire ecosystems, the distribution of their areas and shapes in the boreal landscape has hardly been analyzed, particularly when compared to similar efforts for lakes (e.g., Cael & Seekell, 2016; Englund et al., 2013; Gardner et al., 2019). This lack of information has restricted the spatial understanding related to mire properties, such as biodiversity and peat carbon storage (Sjöström et al., 2020), and the upscaling of these processes to larger spatial scales. For example, while small mire patches or laterally merged mires with more complex shapes might favor plant species richness through stronger edge effects (Howie & Meerveld, 2011), birds might be favored by open areas and low tree height, often associated with larger mires (Fraixedas et al., 2017). Furthermore, increased representation of edges in mires with more complex shapes might result in lower carbon accumulation due to better aeration and, hence, decomposition at the edges (Nordström et al., 2022). Even though it is well established that topography and landscape position regulates the water balance and flowpaths, the links between site-specific mire area and shape distributions and the surrounding catchment areas have rarely been addressed at larger spatial scales and for different land surface ages.

To fill this knowledge gap, the present study aims at exploring mire size-distribution patterns and identifying key drivers that shaped the present morphology and patterns of mires over a 30 km transect located in northern

Sweden. The transect corresponds to a post-glacial mire-chronosequence, which enables us to simultaneously study mire size distribution at the landscape level, and across the Holocene time-scale (Ehnvall, Ratcliffe, Bohlin, et al., 2023). Fennoscandia was covered by the 3 km thick Scandinavian Ice Sheet during the last glacial maximum 26.5–20 thousand years ago (Clark et al., 2009; Stroeven et al., 2016). The weight of the ice sheet compressed the Earth's crust, and following the glacial retreat, isostatic rebound resulted in the emergence of new terrestrial land areas along the coast of the Bothnian Bay (Påsse & Daniels, 2015). This uplift facilitated primary mire formation and expansion (Ehnvall, Ratcliffe, Bohlin, et al., 2023), forming the basis for the mire chronosequence applied in the present study. In addition, weathering of mineral soils after land exposure from the sea (Starr & Lindroos, 2006) resulted in mineral nutrient gradients across the chronosequence, impacting mire productivity (Ehnvall, Ågren, et al., 2023). Our mire chronosequence approach is based on this isostatic land uplift, where the highest possible mire age corresponds to the specific land surface age (time since emergence from the coast). Accordingly, coastal mires are younger, while mires further inland represent older successional stages. We explored the added influence of topography (using local and regional geomorphic attributes) on mire development across multiple scales, ranging from the broad regional and catchment scales down to individual mires and their surrounding areas. More specifically, we assessed (a) if mire coverage and abundance increase with land surface age, (b) if older parts of the landscape are characterized by larger, more complex mire shapes compared to younger parts of the landscape, (c) if the mire lateral expansion is controlled by catchment setting including size, wetness and slope and (d) if landscape slope and wetness can explain mire size distributions.

2. Materials and Methods

2.1. Study Area

We studied temporal patterns in mire lateral extent and configuration over the Holocene time scale using the 24 km wide Sävar Rising Coastline Mire Chronosequence (SMC) located in the Swedish county of Västerbotten in the Bothnian Bay Lowlands (BBL; Figure 1). Since deglaciation of the Scandinavian Ice Sheet ∼10,000 years before present (BP; Stroeven et al., 2016), land areas in this region are continuously rising from the sea due to post-glacial isostatic rebound. The current isostatic rebound maximum of the Scandinavian Ice Sheet (9 mm yr^{-1}) is located close to the SMC (Påsse & Daniels, 2015), where land is exposed from the sea at one of the highest rates globally (Nordman et al., 2020). Because of the high rebound rate as well as favorable climatic, geomorphological and hydrological conditions, the SMC has formed within a constrained distance from the present coastline (∼30 km), corresponding to a land surface age of ∼9,000 years BP (Figure 1). In Ehnvall, Ratcliffe, Bohlin, et al. (2023), we provide further details about the chronosequence approach and compare the SMC to other regional chronosequences.

The 30-year annual, as well as July and January monthly averages for temperature and precipitation in the SMC during the 1991–2020 reference period, were 3.5, 15.7, −6.8°C and 654, 79 and 48 mm (Swedish Meteorological and Hydrological Institute). Values were obtained by averaging observations from coastal (Umeå Airport) and inland (Vindeln-Sunnansjönäs) meteorological stations closest to the SMC. The landscape morphology is characterized by elongated ridges of glacial till interlaid by valleys of deposited postglacial clay, silt, and sand (Lindén et al., 2006). Lacustrine and glacio-lacustrine sediments border the river Sävarån, which traverses the study area. Paragneiss, predominately made of quartz, mica and feldspar, dominates the area, but mafic (basaltic andesite, gabbrodiorite) and felsic (granodiorite, granite) rock intrusions are also present, according to bedrock maps (1:50,000) by the Geological Survey of Sweden. The area lies in the southern mixed mire region (aapa mire sub-region) and is dominated by minerogenic mires (fens; Gunnarsson et al., 2014).

2.2. Study Approach

We derived a number of metrics (Table 1) to characterize individual mire morphometry (“mire”), and terrain indices linked to their surrounding buffer area within a 20 m distance (“buffer”), and to the upslope contributing area (“catchment”). To assess how mire morphometry and abundance relate to large-scale topographic variation and land-surface age across the SMC, we used land-surface-age-classes spanning one-thousand years each. In each age-class, we analyzed the topography of non-mire upland areas, which are mainly occupied by mineral soils (Ågren et al., 2022). According to the Swedish property map (Swedish Mapping, Cadastral and Land Registration Authority), the land cover/land use in the upland areas is predominately coniferous forest, while deciduous forests,

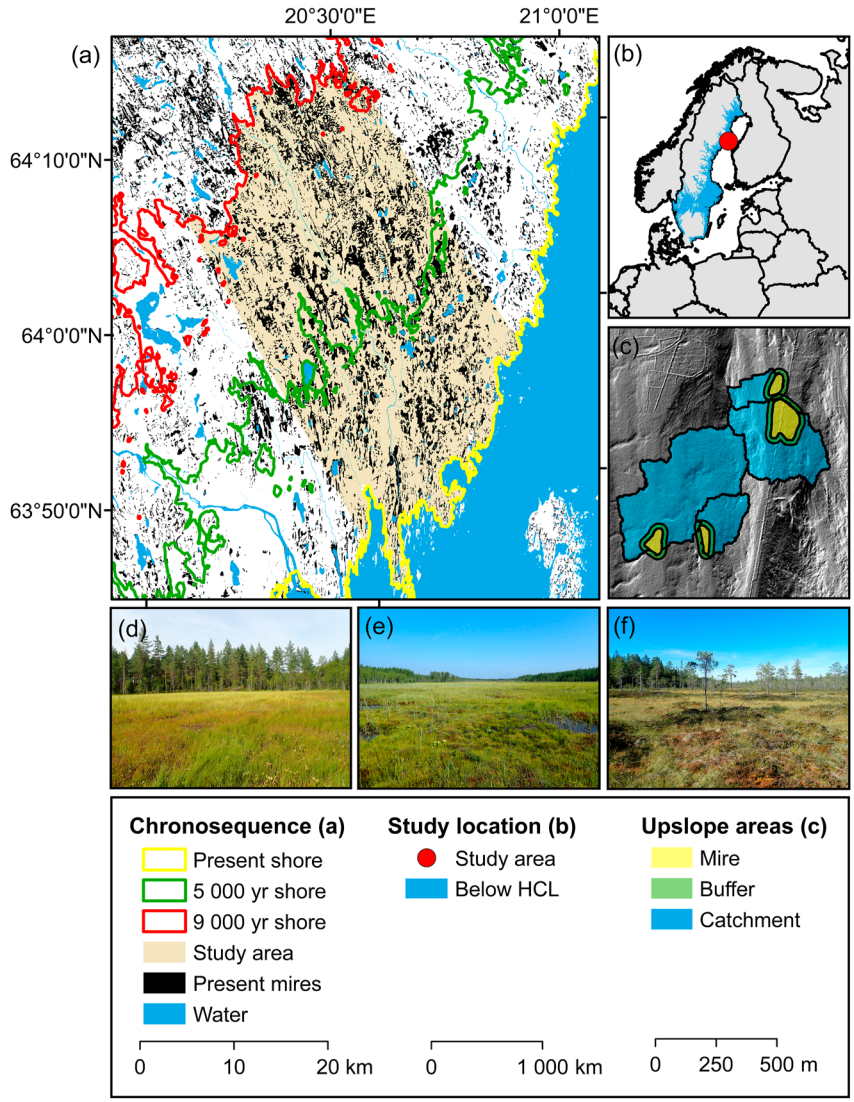

Figure 1. (a) The mire dense Sävar Rising Coastline Mire Chronosequence (SMC) is located below the highest coastline in the 0–170 m above sea-level elevation range in northeastern Sweden (b). Historical shorelines (9,000 and 5,000 years BP) are shown together with the present shoreline. Areas below the highest coastline (HCL) are marked in the national map of Sweden (b). Panel (c) shows the study design with the mire area (yellow) and the 20 m wide upland soil surrounding the mire (buffer, green) as well as the full upland soil catchments (blue) for four young mires. A 2 m gridded hillshade illustrates the variation in local topography. In panels (d–f), three mires from the chronosequence area are shown, where (d) represents a young mire, (e) an intermediate-aged mire, and (f) an old mire located at land surface ages of ca 600 years, 2,600 and 4,000 years, respectively.

settlements, infrastructure and other open areas can be found in smaller parts of these areas. By using slope and soil moisture estimates at the different scales ("mire," "buffer," "catchment" and "land-surface-age-class"), we evaluated whether upland topographic constraints on mire extent varied with scale or land-surface-age.

2.3. Selection and Pre-Treatment of Mire Objects

We based mire distribution patterns on the extent of mires in the Swedish Property Map (Swedish Mapping, Cadastral and Land Registration Authority). This map provides the most detailed mire information currently available in the SMC. The aerial-photo-based mire map includes both mires that are geographically isolated from larger rivers as well as those on floodplains. In this study, we excluded 4 mires out of 3,060 total because they were located directly along the Sävarån, which drains a catchment area of 1,163 km^2. The total area of

Table 1
Mire and Upslope Characteristics

Variable (unit)	Description	Source
Age (years BP)	Mean mire age based on land surface age	DEM[a] and shore displacement curve, Equation 1 [b]
Land-surface-age-class (years BP)	1,000-year age classes including all land covers	DEM[a] and shore displacement curve, Equation 1 [b]
Mire area (km^2)	Total mire area	Property map[a]
Mire shape index	Quotient between the perimeter of a circle and the true mire perimeter for a given area	Property map[a] and Equation 2 [c]
Total mire coverage (%)	Percentage mire coverage within each 1,000 years land-surface-age-class	Property map[a], DEM[a] and shore displacement curve, Equation 1 [b]
Mire abundance (count per km^2)	Number of mires per 1,000 years land-surface-age-class area	Property map[a], DEM[a] and shore displacement curve, Equation 1 [b]
Cumulative percentage of total mire area (%)	Cumulative mire area per land-surface-age-class sorted from smallest to largest mires, normalized to total mire area in the age class	Property map[a], DEM[a] and shore displacement curve, Equation 1 [b]
Cumulative percentage of mire count (%)	Cumulative number of mires per land-surface-age-class, normalized to total number of mires in the age class	Property map[a], DEM[a] and shore displacement curve, Equation 1 [b]
Cumulative mire abundance (count per km^2)	Cumulative number of mires per land-surface-age-class, normalized to age class area	Property map[a], DEM[a] and shore displacement curve, Equation 1 [b]
Catchment-to-mire area ratio (m^2 per m^2)	Areal ratio between the unique upslope catchment area and the mire area	Property map[a], DEM[a], Equation 3
Slope (%)	Median mire, buffer and catchment slope	DEM[a], slope function[d]
SMI	Soil moisture index describing the likelihood (%) of moist surface conditions	Soil moisture map[e]

Note. The spatial resolution of all variables is 2 × 2 m, except for indices based on mire area, which are object based (1:10,000).
[a]Swedish Mapping, Cadastral, and Land Registration Authority. [b]Renberg and Segerström (1981). [c]Forman and Gordon (1986). [d]Zevenbergen and Thorne (1987). [e]Swedish University of Agricultural Sciences.

these floodplain mires was 3.6 km^2. This decision reflects our focus on the non-floodplain mires, which are the dominant type in this region, and for which fluvial factors such as erosion or deposition are not relevant (Lane et al., 2018).

Before testing our research questions, we first merged mire segments divided by smaller roads. Secondly, we considered open water patches within mires to be mire ponds and, thus, part of the mire. On the other hand, we treated patches of mineral soil within mire objects as holes in the mire polygons, since they are part of the supporting mineral soil in the mire catchment. Generally, the property map covered mires with an area extending 2,500 m^2, while smaller mires were only sporadically mapped. To avoid bias toward parts of the SMC with more comprehensive mapping of small mires, we excluded all mires with an area of <2,500 m^2. Performing these steps resulted in 3,056 individual mire objects in the SMC. Photos from a selection of SMC mires can be found in our interactive mire map (https://slughg.github.io/MiresChrono/).

2.4. Land Surface Age

We combined a 2 × 2 m national gridded digital elevation model (DEM) with a local shore displacement curve (Equation 1; Renberg & Segerström, 1981) to calculate mineral soil surface age (T_{age}). The 2 × 2 m DEM was generated by the Swedish Mapping, Cadastral and Land Registration Authority from LiDAR scanning (0.5–1 points m^{-2} point density, 0.3 m vertical and 0.1 m horizontal resolution). The shore displacement curve was based on varved lake sediments from six lakes in the 29–177 m above sea level (m.a.s.l.) elevation range, allowing for both identifying the transition from marine to lacustrine sediments and to date this transition. Based on the extent of the shore displacement curve, we set the upper limit of the SMC at 170 m.a.s.l. Land surface age (T_{age}) was calculated on a pixel basis from the 2 m DEM (z) using Equation 1.

$$T_{age} = -0.287z^2 + 99.967z \quad (1)$$

We grouped mires in the SMC into nine 1,000-year age-zones based on the average land surface age for each mire. Additionally, the age raster was used to classify the SMC into nine 1,000-year age intervals. The areas of the age intervals ranged between 64 and 137 km^2, and the number of individual mire objects varied in the 223–626 range between the age classes (Table S1 in Supporting Information S1).

2.5. DEM Pre-Processing, Catchment and Buffer Delineation

From the 2 × 2 m DEM, we delineated mire catchments using the open-source GIS system Whitebox Geospatial Analysis Tools. Before catchment delineation, the DEM was hydrologically pre-processed in three steps. First, streams on agricultural land, as defined in the Swedish property map, were burned 1 m into the DEM. Second, road and stream intersections were carved into the DEM. Finally, sinks were removed from the DEM using the breaching algorithm developed by Lindsay (2016). These pre-processing steps are necessary (Lidberg et al., 2017) since the road network, ranging from highways to small forest roads, is well developed and affects surface flow paths in most of the study area.

We defined the catchment area of mire as the upslope area that is hydrologically connected to the mire through flow paths that supply water and solutes. The total contributing area covers both upslope areas on mineral soil and any upslope mires. If upslope mires constitute parts of the total contributing area, they can intercept water and nutrient flows from upslope areas before they reach downslope-located mire (Cohen et al., 2016). To account for this, we derived unique catchment areas, which hereafter are the focus of the paper, and are referred to as the "catchment" (Ehnvall, 2023). These areas represent the upslope contributing area that a downslope-located mire does not share with other mires. We calculated unique catchment areas based on a mire corrected flow pointer map, where all mires in the hydrologically pre-processed DEM were assigned the value 0, thus making them hydrologic sinks. From the mire-corrected DEM, flow direction and flow accumulation were calculated using the deterministic eight-direction flow model (D8; O'Callaghan & Mark, 1984). Finally, we extracted catchments, where the total mire polygon was assigned as the catchment outlet. Thus, all upslope flow paths that pass through the mires are included in the contributing area.

While the upslope contributing area is a useful proxy for the regional influence of topography on mires, it is not sufficient for characterizing local conditions close to the mire edge. The characteristics of the mire margins are, however, important to consider because they represent the area allowing for growth and expansion of the mire (Ehnvall, Ratcliffe, Bohlin, et al., 2023; Ruppel et al., 2013). To describe conditions closest to the mire edge, both up- and downslope of the mire, we extracted 20 m wide buffers surrounding each mire object (Figure 1).

2.6. Mire Geometry and Terrain Indices

Mire area and the shape index (Equation 2) were used to quantify mire morphology. The shape index is a measure of the complexity of mire's two-dimensional shape (Equation 2; Forman & Gordon, 1986), which compares the perimeter (P) of the mire with the perimeter of a circle with equal area (A). A circular mire has the largest interior area compared to its perimeter and the more the shape index deviates from 1, the more the shape deviates from a circle. In addition to describing the complexity of the two-dimensional mire shape, we also obtain an estimate of possible edge effects on mire biodiversity using the shape index.

$$\text{Shape index} = \frac{2 * \sqrt{A} * \pi}{P} \tag{2}$$

The influence of upslope locations on the hydrological and biogeochemical functioning of mire can be assumed to be related to the size of the area (Pilgrim et al., 1982). Thus, the ratio of upslope contributing area divided by mire area has been suggested as an indicator to characterize hydro-geochemical and ecological functions of mires (Lane et al., 2018). We calculated the catchment-to-mire-ratio by dividing the area of the delineated unique catchment by the area of the mire (Equation 3).

$$\text{Catchment} - \text{to} - \text{mire ratio} = \frac{\text{Catchment area}}{\text{Mire area}} \tag{3}$$

Indices related to topography and hydrology were assessed locally and regionally by aggregating them at the mire-, buffer- and unique-catchment-scales. In addition, at the largest spatial scale (land-surface-age-classes), we

described the topography and hydrology of non-mire areas by masking out mires from the age classes. Terrain slope and a recently developed national soil moisture index (Ågren et al., 2021) were used to quantify topographic and hydrologic conditions. We chose terrain slope, since it is a widely-used, primary terrain index. High values correspond to steep slopes, which can indicate the presence of physical constraints that mire needs to overcome before expanding further upland. In a wider context, terrain slope also indicates the hydrologic conditions at the site and it may indicate flow direction as well as drainage conditions. Slope (%) was calculated in SAGA GIS 7.9.0 from the 2 × 2 m DEM according to Zevenbergen and Thorne (1987).

The soil moisture index (SMI) was chosen as a complement to the terrain slope since it is currently the most accurate soil moisture index in Sweden (Ågren et al., 2021). The SMI is less commonly used than terrain slope, and more difficult to derive since it is based on machine learning techniques relying on a series of input variables such as terrain indices (e.g., slope, depth-to-water, topographic wetness index, topographic position index), Quaternary deposits and soil depth, as well as ancillary data covering runoff and climate data (Ågren et al., 2021). The SMI does not include depths of peat or organic soil as input variables, but there is a clear link between the SMI and peat depth (Ågren et al., 2022). The SMI describes the likelihood (0%–100%) that a pixel in the map is wet. Correspondingly, high values indicate wet conditions, which are favorable for lateral mire expansion (Ehnvall, Ratcliffe, Bohlin, et al., 2023). The SMI was available in the form of a 2 × 2 m raster.

2.7. Data Aggregation and Analysis

The number of mire objects and the total mire area within each land-surface-age-class was calculated, and from these mire abundance and coverage were extracted based on the total area of the age classes. Further, to illustrate the representativeness of differently sized mires to the total mire area, we grouped mires into four area-classes of <0.01 km^2, 0.01–0.1 km^2, 0.1–1 km^2, and 1.0–10.0 km^2 (note the logarithmic scale), and explored how the mire area groups changed across the age classes.

For each of the mire area classes as well as for the upslope features (buffers, catchments and non-mire areas in the land-surface-age-classes), we extracted median and interquartile ranges (IQR = 75th percentile–25th percentile) of slope and SMI. We compared the topographic variation in the upslope features as a driver of mire distributions using slope and SMI estimates. All statistical analyses were performed in R version 4.0.3 (R Core Team, 2020).

3. Results

3.1. Mire Abundance and Coverage Across Land-Surface-Age-Zones

We found a parabolic relationship between mire abundance and land-surface-age-class (R^2 = 0.82, p < 0.01; Figure 2a) in the SMC, with the lowest abundance (1.8 mires per km^{-2} based on ∼220 mire objects) in the 5,000–6,000 years BP class. In the youngest class (0–1,000 years BP), mire abundance was 6.8 mires per km^2 (∼450 mire objects) and in the oldest class (8,000–9,000 years BP) 4.6 mires per km^{-2} (∼630 mire objects). In contrast, mire coverage increased continuously from the youngest land-surface-age-class (∼14%) to the 6,000 years BP class (∼33%), but fluctuated around 30% in the 6,000–9,000 years BP interval (R^2 = 0.77, p = 0.01; Figure 2b).

We explored the contrasting pattern in mire abundance and coverage by comparing distributions of different sized mires between the age classes (Figures 2c and 2d). Mires belonging to the largest area group (>1 km^2) emerged in the 1,000–2000 years BP land-surface-age-class at >1.9 km from the coast. The number and area of these large mires increased over time in the 2,000–9,000 years BP range. Despite being few in number, the largest mires (>1 km^2) accounted for a considerable part of the total mire area within the age classes. For example, in the 6,000-year land-surface-age-class, the six largest mires, out of the total ∼260 mires, had an individual mire area of >1.5 km^2 and together accounted for ∼66% of the total mire area within the age class. Small mires (<0.01 km^2) remained high in number throughout the SMC, but individual small mires accounted for less than 0.1% of the total mire area within any land-surface-age-class. The coverage of the largest mires (1.0–10.0 km^2) increased over time until 6,000 years, while the coverage of the two smallest area groups (<0.01 km^2 and 0.01–0.1 km^2) decreased over time. The coverage of mires in the 0.1–1.0 km^2 group remained fairly constant across age zones (Figure 2d).

We further found that the time since land emergence from the sea influenced the cumulative mire area as well as the cumulative number of mires. In the youngest two age classes, ∼75% of all mires accounted for ∼30% of the

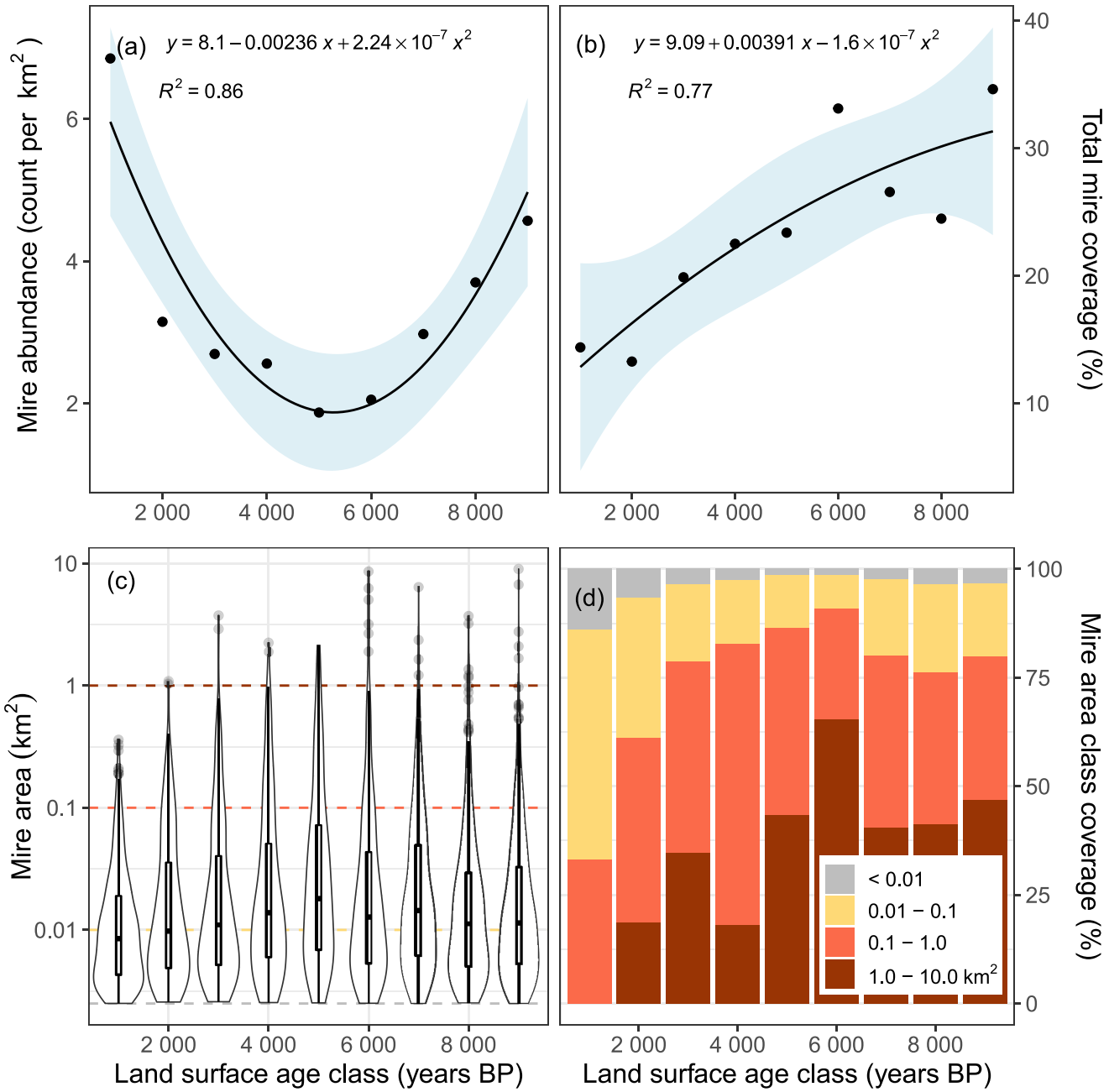

Figure 2. Mire abundance (a), coverage (b), the distribution of individual mire areas (c) and total mire area (d) of different area classes (<0.01 km^2, 0.01–0.1 km^2, 0.1–1 km^2, and 1.0–10.0 km^2) across land-surface-age-classes. Shaded areas in (a) and (b) represent the 95% confidence intervals of the applied functions. Dotted lines in (c) mark area classes applied in (d). Mire coverage and abundance were calculated relative to the total age class areas.

mire area, while in the older age zones 75% of the mires accounted for <20% of the total mire area (Figure 3a). In the oldest age zone, the largest six mires accounted for ~50% of the total mire area within the age zone (Figure 3b).

3.2. Mire Shape and Catchment Area Ratios Across Land-Surface-Age-Classes

Across all land-surface-age-classes, mire shape-complexity tended to increase with increasing mire area (Figure 4a). Especially, mires of the largest area group (1.0–10.0 km^2) had higher shape indices, around 6–7, suggesting more complex shapes compared to the smaller mires with shape indices below 4. These larger mires with more complex shapes emerged after ~2,000–3,000 years BP. However, within the two smallest area groups,

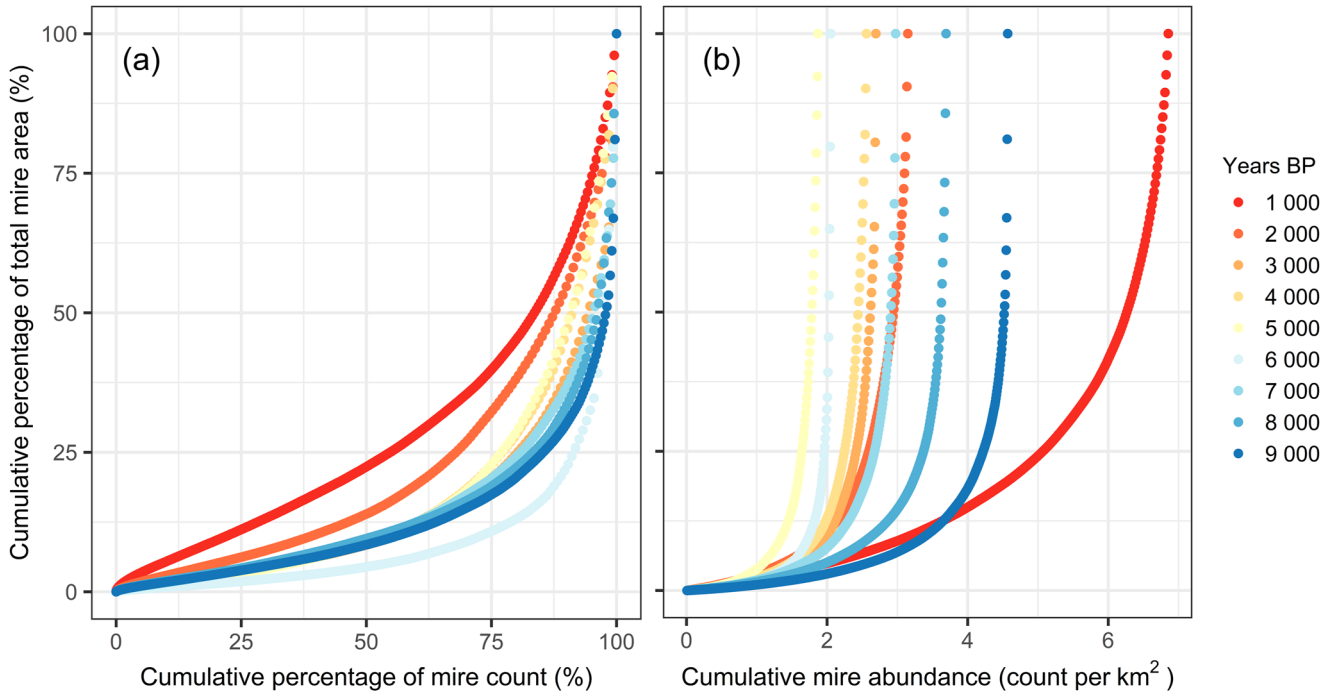

Figure 3. The cumulative percentage of total mire area in relation to the cumulative percentage of mire count (a) and the cumulative mire abundance (b), sorted from the smallest to the largest mires. Land surface age zones are marked in different colors. Only a few large mires account for most of the mire area within the land surface age zones. For example, the six largest mires in the 6,000 years age zone account for 66% of the total mire area (a).

mires in the youngest land-surface-age-class (0–1,000 years BP) differed from mires in older age zones by having a higher median shape index, and higher variability (higher IQR) in shape-complexity (Wilcoxon-rank-sum test, $p > 0.001$).

We found no clear changes in the catchment-to-mire area ratio over time in any of the mire area classes (Figure 4b). However, in all age classes, the median catchment-to-mire area ratio decreased from the smaller to the larger mires, and exceeded one in all mire area groups. In addition, the class comprising small mires had a larger variability in catchment-to-mire ratios.

3.3. Terrain Slope and Moisture as Drivers of Mire Abundance

We found significant, positive linear relationships between mire abundance and median slope in non-mire areas of the land-surface-age-classes ($R^2 = 0.8$, $p < 0.01$), as well as between mire abundance and the interquartile range of soil moisture index (SMI; $R^2 = 0.77$, $p < 0.01$) in non-mire areas of the age classes (Figure 5). The youngest age class deviated from this general trend by showing a much higher mire abundance than expected, which likely reflects the scattered initiation of mires on young surfaces and temporal restriction of lateral expansion. The youngest land-surface-age-class was excluded from the regression analysis as it deviated from the remaining mire population.

In terms of slope and soil moisture conditions, we found differences in relation to land-surface-age-class between mires on the one hand, and catchments and buffers on the other (Figure 6). Mire areas were flatter (slope <4%) and moister (SMI > 90) compared to catchment areas. Buffer slope and soil moisture conditions represent intermediate conditions between mire-covered areas and the surrounding catchment. Within the studied mire population, the median mire slope decreased with an increasing mire area. Likewise, the median mire wetness increased with larger mire areas.

4. Discussion

4.1. The Importance of Landscape Aging on Mire Patch Distributions

Our analysis revealed systematic landscape-scale changes in the distribution and shape of mire ecosystems over 9,000 years of post-glacial succession. Importantly, for the Sävar Rising Coastline Mire Chronosequence (SMC),

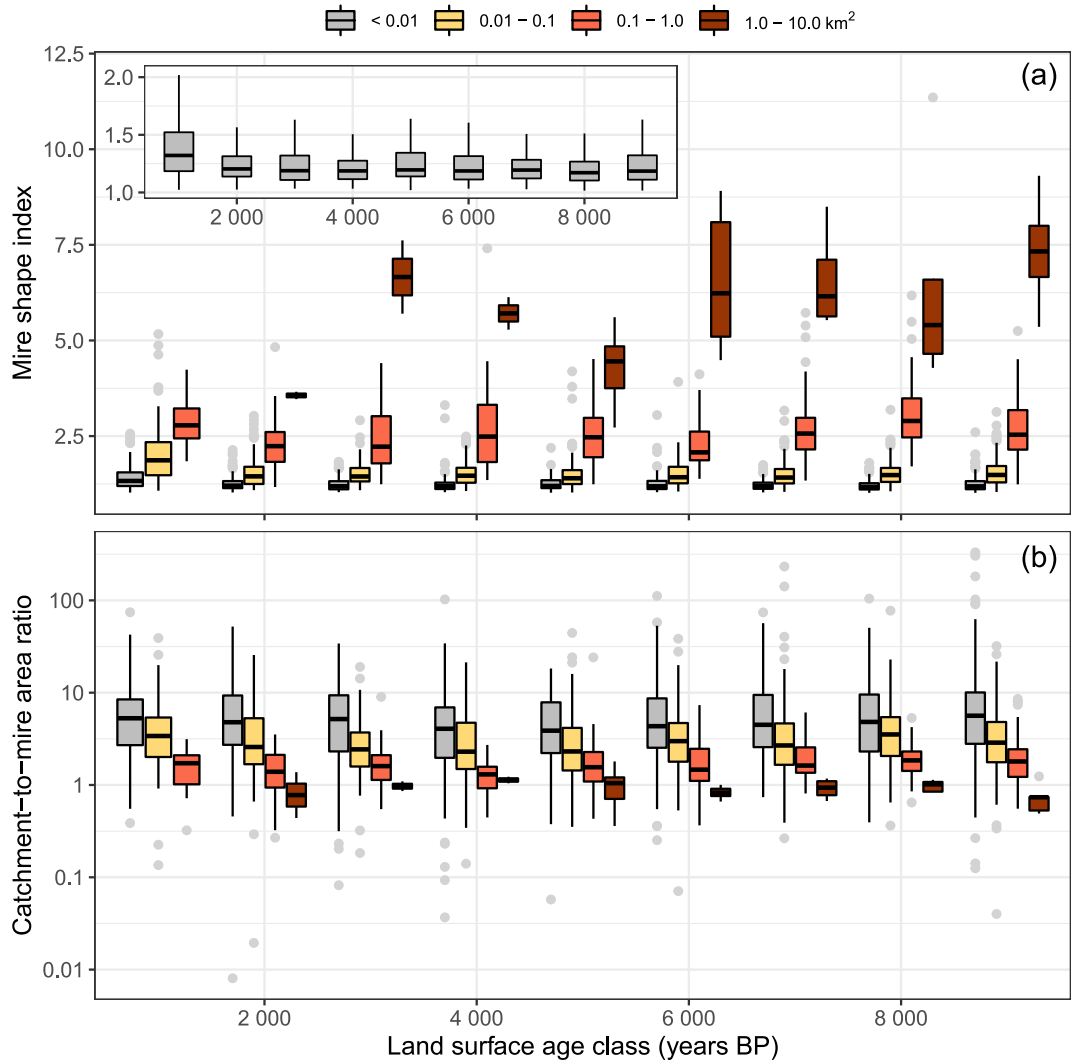

Figure 4. Mire shape index (a) and catchment-to-mire area ratio (b) across mire area groups (0–0.01 km^2, 0.01–0.1 km^2, 0.1–1 km^2, and 1.0–10.0 km^2). In panel (a), the smallest area group is displayed (without outliers) in the plot inset. The catchment-to-mire area ratio (note the logarithmic scale) was based on the unique upslope catchment area, which is the upstream drainage area of a mire that is not shared by any other upstream mires.

large mires (>1.0 km^2) accounted for a considerable portion of the total mire area, despite being few in number (Figure 2d). Further, as large mire complexes formed in older parts of the SMC, the landscape mosaic became more mire-dominated (>30% mire cover, Figure 2b). Our estimated mire cover for the SMC is slightly higher than average in comparable sites in the region (<20% mire cover), but is similar to estimates from northern parts of the Bothnian Bay Lowlands (BBL; Ehnvall, Ratcliffe, Bohlin, et al., 2023). Thus, given the similar climatic conditions over the Holocene, the high mire coverage in the SMC suggests suitable conditions for mire initiation and lateral expansion, possibly combined with lower impacts of anthropogenic land use changes that are known to alter mire area elsewhere in this region (Norstedt et al., 2021). Geological factors, including uplift and fluvial processes, have also been suggested as primary drivers for peat initiation in the Hudson Bay Lowlands (HBL) in Canada (Glaser, Hansen, et al., 2004; Glaser, Siegel, et al., 2004). Similarities with our conclusion are hardly surprising: both regions are centered in climatic regions ideally suited for peat formation, such that wetness and land availability for mire formation are primarily controlled by non-climatic factors.

Despite the increase in mire coverage since land emergence from the sea, the abundance of small mires did not change accordingly along the chronosequence (Figure 2a). Instead, small mires alone dominated the youngest parts of the SMC, while a heterogeneous mixture of small mire patches together with larger mire complexes

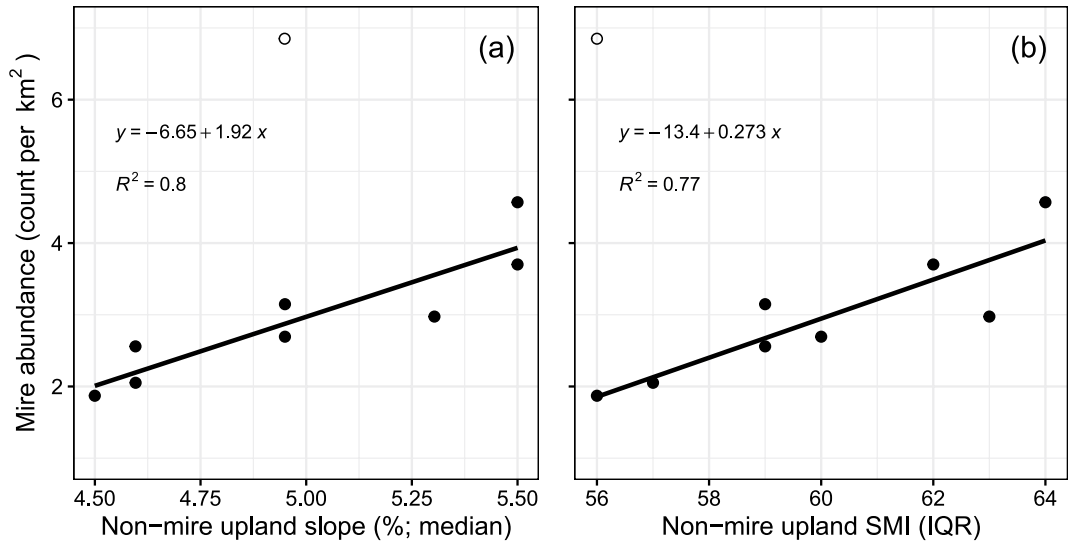

Figure 5. Positive, linear relationships between mire abundance and the median slope (a), as well as the interquartile range of soil moisture (b; SMI) in non-mire areas of the land-surface-age-classes. Non-mire areas were defined as all areas within an age class that are not covered by mires and thus, represent mire controls at the largest spatial scale. The youngest land-surface-age-class (unfilled circle) was excluded.

characterized the older end of this chronosequence (Figure 2). Interestingly, small mires found in younger parts of the landscape had more complex and varied shapes when compared to those in older parts of the landscape (Figure 4). These temporal patterns reflect distinct mire initiation and expansion pathways in different parts of the chronosequence (Stum-Boivin et al., 2019). Accordingly, in the youngest parts of the landscape, the primary mire formation has likely been the dominant initiation process, similar to that suggested for east-BBL (Huikari, 1956). The primary mire formation along exposed bays can lead to more elongated shapes, rendering higher shape indices compared to mires initiated through terrestrialization or paludification. The shapes of mires formed through primary mire formation or terrestrialization likely remain simple as lateral expansion proceeds, whereas continued expansion on flat areas through paludification can give rise to more complex shapes (Figure 4a). This is also consistent with the theory that the shape complexity and mire size are expected to increase as peat progressively expands into hydrologically suitable areas, circumventing drier ridges (Ehnvall, Ratcliffe, Bohlin, et al., 2023).

While established mires may merge to form larger mire complexes in landscapes old enough to have sufficient lateral peat accumulation rates, new mires with relatively simple shapes can continue to initiate through terrestrialization or paludification. This is possible because the lateral mire expansion through paludification often requires smaller water input from the catchment and can thus proceed in locations that were not available for primary mire formation (Kulczyński, 1949; Ruppel et al., 2013). The inherent differences in mire initiation and expansion rates (Ivanov, 1981) along the chronosequence likely contributed to the higher diversity of mire size found in old parts of the SMC. While such mechanisms remain to be tested, our analysis highlights key changes in mire shape, which are known to influence the ecology and functioning of these ecosystems and the landscapes they occupy (Rehell et al., 2019).

4.2. Mire Area Distributions in Relation to the Hydrological Upslope Catchment Support

The upslope area determines minerogenic mire persistence by regulating the supply of water and nutrients (Sallinen et al., 2023). The ratio between the non-mire and mire areas decreases within a catchment as minerogenic mires expand into more easily accessible depressions and plains (Ehnvall, Ratcliffe, Bohlin, et al., 2023), and the non-mire catchment area progressively becomes restricted to drier areas, including steep slopes and ridges. For the SMC, we observed a decrease in this ratio with mire size across all land-surface-age-classes, stabilizing at ~1:1 in the largest mires (>1.0 km^2; Figure 4b). A minimum catchment-to-mire area ratio should define the limit of persistence of minerogenic mire. For mires with equal internal controls on their hydrologic regimes, those with stronger hydrological catchment support are likely to be more resilient toward drought when

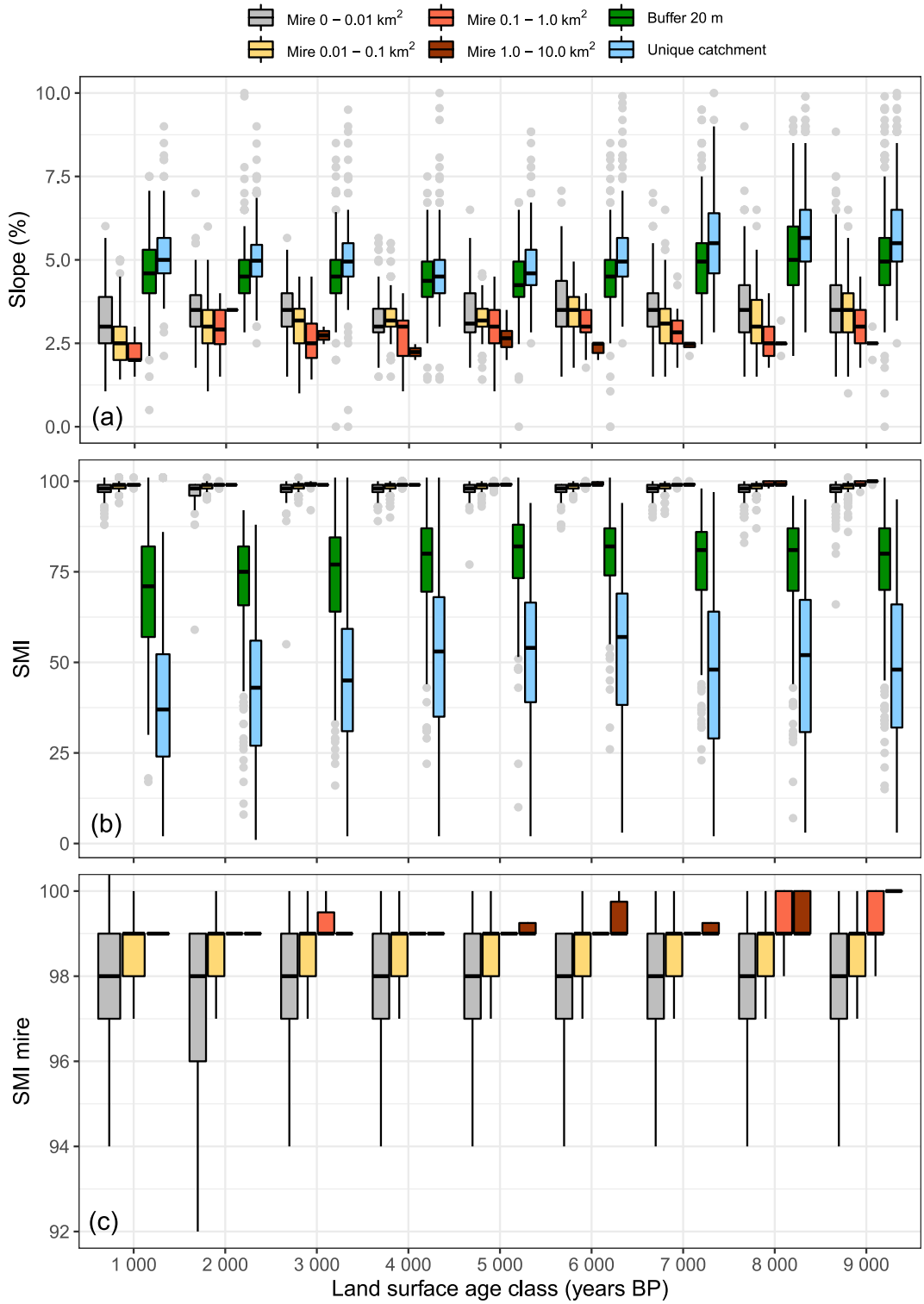

Figure 6. Median slope (a) and median soil moisture (b; SMI) across mires, buffers and unique catchments. Panel (c) shows a zoomed in version of mire soil moisture scores, with no outliers displayed.

compared to those with weaker catchment support (Lambert et al., 2022). If a mire expands beyond the hydrological support capacity of the catchment, that is, in this study below the 1:1 ratio, lateral peat expansion might be inhibited by drought. At its extreme, this can lead to shrinkage or potentially loss of the mire area (Gallego-Sala

& Prentice, 2013; Velde et al., 2021) as can be observed today in relic peatlands at or beyond the present climatic limit for specific peatland types (Chico et al., 2019; Luoto & Seppälä, 2000; Moar, 1956; Silva et al., 2019). Under wetter climatic conditions, the catchment-to-mire ratio could decrease, but still be sufficient for mire maintenance (Sallinen et al., 2023). Importantly, however, mires are resilient systems that, because of the low hydrologic conductivity of highly decomposed peat, can maintain elevated water tables and even saturate surrounding areas (van Breemen, 1995). Hence, mires with deep peat layers can sustain high water tables even under drought conditions, whereas mires with shallower peat may experience greater water table fluctuations (Lambert et al., 2022; Moore et al., 2021). Based on this, the external influence from catchment inputs and internal controls over the mire water balance likely interact to determine the vulnerability of minerogenic mires to changing climatic and hydrological conditions (Lambert et al., 2022).

Interestingly, small mires in the SMC were more variable when it came to the catchment-to-mire ratio compared with larger mires (Figure 4b). This cannot only be caused by a reduced upper catchment-to-mire ratio limit in larger mires since mire shape complexity also increases with area (Figure 4a). Instead, small and shallow mires can probably remain wet despite low catchment-to-mire ratios (close to 0:1) because of their limited basin volume, which can be recharged even from a small upslope catchment area (Winter, 1988). Also, groundwater intrusions from below (Jaros et al., 2019; Kulczyński, 1949; Lambert et al., 2022) might compensate for the small upslope contributing area, at the same time as tree sheltering reduces water loss through evaporation (Limpens et al., 2014). At the other extreme, small mires can persist under the support of very large upslope catchment areas (up to 18:1). Such large catchment support relies on sufficient discharge from distinct mire outlets (Sirin et al., 1998) or more often, from wider diffuse outlet zones (Sallinen et al., 2019). In addition, seepage to aquifers at mire margins may also contribute to water loss from these systems (Hokanson et al., 2020; Kulczyński, 1949; Marttila et al., 2021). The wide range in the catchment-to-mire ratio in the smallest two area groups suggests that these mires exhibit a more variable range of hydrological conditions due to their greater external catchment area and thus greater dependency on non-mire hydrology compared to larger mires. In contrast, larger mires with smaller catchment-to-mire area ratios are more likely to be dependent on internal controls and less on external hydrological conditions. We argue that this might be an additional reason why parts of the mires remain small throughout the land-surface-age-classes (Figure 2), whereas large mires in the SMC have expanded into larger portions of their catchments and decreased the catchment-to-mire ratio to <2:1 for all mires in the largest area group (1.0–10.0 km^2).

At its extreme, mire lateral expansion could hypothetically drive the catchment-to-mire area ratio to approach 0:1, resembling ombrogenic conditions. From a strict hydrological perspective, ombrogenic mires exist in flat landscapes where their water tables can rise above the surrounding land area, ensuring that the mire receives water and nutrients exclusively from precipitation. In the present study, we used a unique catchment area to express the catchment-to-mire area ratio, since we considered this representation to be more reflective of catchment nutrient supply compared to the total catchment area including any/all upslope mires (Liu et al., 2020). However, no mires in this area had ratios of ∼0:1 even when the total upslope catchment area was considered (Figure S1 in Supporting Information S1). Thus, hydrologically, the SMC strictly supports only minerogenic mires. This is in line with the general conception of the northern limit to ombrotrophic mires in Sweden, widely regarded as being ∼500 km south of the SMC, in Bergslagen (Almquist-Jacobson & Foster, 1995). Isolated patches of marginally ombrotrophic mires do, however, exist north of this limit, much closer to our study area (Taveljömyran ∼30 km southwest of the SMC in Granlund, 1932), and ∼70 km east of the SMC in the Ostrobothnia region in Finland (Sallinen et al., 2023). Differences in landscape slope and topography between the east and west flanks of the BBL may explain why ombrogenic mires form at similar latitudes in Finland but not in Sweden. Our results on the lower limits of the catchment-to-mire area ratio, and its regulation of the mire extent can potentially improve process-based (Treat et al., 2022) or TOP-models (Kleinen et al., 2012) used to model peat accumulation in minerogenic mires. Such models often rely on assumptions based on ombrogenic systems, and currently provide incomplete representation of minerogenic systems. Noteworthy, the terrain indices and catchment-scale approach applied in the present study are by no means restricted to uplift areas unless long-term trends are in focus. Hence, the present catchment support to mires can be studied by applying similar spatial analyses in areas outside isostatic rebound zones.

4.3. Landscape Slope and Wetness as Drivers of Mire Size and Shape Configuration

Soil moisture conditions (Figure 6c) and weathering derived nutrients regulate mire productivity (Ehnvall, Ågren, et al., 2023) and regulate peat lateral expansion in the SMC (Ehnvall, Ratcliffe, Bohlin, et al., 2023). The lower

limit in the catchment-to-mire ratio (1:1) itself is unlikely to be a purely hydrological constraint that limits mire expansion and size. Rather is the lower bound of the catchment-to-mire ratio in the SMC determined by regional topo-edaphic controls, which prevents peat from occupying the whole catchment (Ehnvall, Ratcliffe, Bohlin, et al., 2023) by physically separating mires from the remaining sloping or otherwise dry ground. The observed increase in median upland (catchments, and within these, buffers) moisture conditions with increasing time since land emergence from the sea, especially in the 0–5,000 years range (Figure 6b), reflects the buildup of thicker humus layers or shallow peat layers surrounding the mires (Ågren et al., 2022). Interestingly, the SMI predicted large mires to be on average wetter than small mires across all land surface age classes (Figure 6c). This supposedly reflects a higher frequency of surface water bodies (e.g., pools or small streams) within or close to larger mires, although this would need to be confirmed. It is important to note that mire moisture conditions based on the soil moisture index should be interpreted cautiously since the mire area itself was included among the input variables when the index was prepared, and since it was primarily developed to describe moisture in forest soils (Ågren et al., 2021).

To complete the conceptual understanding of mire expansion in the SMC, we identified a mire slope limit of ∼4% (∼2° slope) above which mires hardly occurred under present climatic conditions (Figure 5a). Supporting upland areas (catchments and buffers) included surfaces with slopes above 4%, but also some surfaces with lower slopes (>2%). The incline in terrain that mires can inhabit is a direct result of the local water balance (Ivanov, 1981), and it differs between landscapes under different hydrologic regimes. The slope limit in our study area is higher compared to limits reported from southern Sweden (Almquist-Jacobson & Foster, 1995) and Alaska (Loisel et al., 2013). However, in wetter parts of Sweden, such as the west of the province of Dalarna, mires commonly cover slopes of 5%–10%, and up to 14% in some areas (Rydin et al., 1999). In maritime areas, such as on the west coast of Scotland, blanket bogs can be found on slopes up to 20% (Gorham, 1957; Pearsall, 1950). Apart from restricting the mire lateral expansion, steep slopes in the mire surrounding areas can also cause hydrological changes to the mire, including development of macro-pores and preferential flow paths in the deeper peat (Hare et al., 2017; Lambert et al., 2022) or causing larger groundwater inflow (Autio et al., 2020).

We found that small mires were steeper compared to larger mires in the SMC (Figure 6). Small mires often have shallower peat layers and may thus better reflect the underlying topography. In contrast, large mires with deep peat layers cover the underlying topography to a greater extent (Loisel et al., 2013). Furthermore, mires with different sizes might have formed in different parts of the landscape and faced different topographic constraints immediately after their initiation. If the balance in precipitation and evapotranspiration remains the same, areas with a steeper slope will require a substrate with sufficiently low permeability to generate a water surplus needed for peat formation (Ivanov, 1981). Alternatively, peat may advance (very slowly) up steep inclines through the gradual increase in absolute water table depth, which is coupled with the vertical growth of peat (Korhola, 1996). After peat is initiated at steeper sloping sites, the water retention capacity increases and the water table stabilizes, and peat starts to accumulate (Ivanov, 1981; Laitinen et al., 2008; Rydin et al., 2013). It is possible that the wetter conditions observed in larger mires (Figure 6c) are caused by their gentler slopes in comparison to smaller mires, which may limit water flow and form pools as a consequence.

After ∼5,000 years, buffer slopes in the SMC became increasingly steeper (Figure 6), suggesting that mires in older parts of the landscape face increasing topographic constraints. The flatter catchment and buffer slopes associated with younger parts of the landscape (Figure 6) indicate that the small total mire area in young parts of the landscape (Figure 2) must reflect other constraints than topographical, such as temporal restrictions related to the timing and spread of mire initiation, or the rate of lateral expansion (Ruppel et al., 2013). The observed increase in mire abundance after ∼5,000 years (Figure 2a) resulted from a systematic shift in the median upland slope, such that steeper slopes and more heterogeneous soil moisture conditions in upland areas generated higher mire abundance (Figure 5). This confirms that merging individual mires into larger mire complexes is restricted to steep and dry terrain, much in line with previous studies from the area, which have suggested that the most rapid mire initiation and utilization of hydrologically suitable areas occurred within 2,000 years after land exposure from the sea (Ehnvall, Ratcliffe, Bohlin, et al., 2023). In parts of the chronosequence that have been exposed for less than 1,000 years, mire initiation may be strongly restricted due to the short time of land exposure. Apart from the youngest age class, we conclude that mire abundance in the area is primarily driven by topographic controls (Figure 5), while the total mire area increase is a function of time and the formation of large mire complexes (Figure 2).

Comparing our results from the Fennoscandian uplift zone in the BBL with those from similar uplift areas, for instance the HBL (Glaser, Hansen, et al., 2004; Glaser, Siegel, et al., 2004) and the White Sea uplift zone (Kutenkov et al., 2018), highlights the importance of local context in driving patterns of mire development. For example, it has been proposed that the inter-fluvial distance is a major control on peat accumulation in the HBL, determining the elevation of the water table mounds. However, the climate in the BBL is considerably different from that in the HBL. As a result, SMC mires are primarily found on flatter ridges above the rivers and very rarely span inter-fluvial gaps, unlike in the HBL. The Swedish part of the BBL is itself exceptional in that the rebound is occurring at the highest rate known globally (Nordman et al., 2020). Rebound is also occurring in a landscape that is comparatively more rugged than the HBL, with upslope catchment areas supplying mires with water and solutes. Apart from the role of topography, cold, mid and northern boreal climates are generally unfavorable for ombrogenic mires due to the influence of surface and ground water (Almquist-Jacobson & Foster, 1995; Damman, 1986; Foster & Glaser, 1986; Sallinen et al., 2023), which may promote peat decay (e.g., Glatzel et al., 2023). This soligenous water supply may be higher in northern climates due to high precipitation and low evapotranspiration during the autumn and winter period (Sallinen et al., 2023; Sjörs, 1990) compared to drier climates. Soligenous water inputs differ considerably across the landscape, for instance leading to minerogenic mire formation in valley bottoms and promoting ombrogenic mires on ridges (Kulczyński, 1949). In flatter landscapes, such as the HBL, soligenous water also explains the occurrence of minerogenic and ombrogenic mires (Glaser, Siegel, et al., 2004). Contrary to drier climates, where low soligenous water inputs could be expected to limit peat formation and expansion, we found mires more fragmented and smaller with greater hydrological support from the catchment. When the catchment area exceeded the area of the mire, that is, a ratio of 1:1, mires did not typically grow above 1 km^2 in size (Figure 4b). While this largely reflects temporal restriction in the mire lateral expansion in the younger end of the SMC, it is nevertheless consistent with Ehnvall, Ågren, et al. (2023), and Ehnvall, Ratcliffe, Bohlin, et al. (2023) who found large areas of the landscape that were wet enough for mire expansion but for which peat remained absent.

4.4. Uncertainties in the Description of Temporal Patterns in Mire Morphometry

Our results and interpretations are based on the current mire extent in the SMC. Land use changes are known to alter ecosystem patterning in forest landscapes (Rana & Tolvanen, 2021; Sallinen et al., 2019). However, the SMC is sparsely populated, with settlements and agriculture concentrated on coastal and river areas (Sävarån and Täfteån). Agriculture may have led to mire loss in these regions, but its impact on overall mire morphometry or cover across the wider mire population is likely small (Ehnvall, Ratcliffe, Bohlin, et al., 2023). Instead, forestry drainage, a common practice in northern Sweden, is the main activity that could have altered the mire morphometry. While large scale-estimates of mire modification due to drainage still have to be made, it has undoubtedly affected the mires in the SMC. Still, open and sparsely treed mires, which are our focus, are likely less affected than tree-covered mires because forestry drainage primarily targets tree-covered peatlands. Finally, mire margin drainage, which is another common practice in the area, may constrain the future lateral mire expansion but has limited influence on the present mire configuration (Bring et al., 2022).

Our chronosequence study compares mire morphometry across zones that emerged from the Bothnian Bay since deglaciation of the Scandinavian Ice Sheet ~10,000 years ago (Stroeven et al., 2016). While land surface age corresponds to the potential maximum mire age, it is important to acknowledge that actual mire age is likely less if mire initiation lags land availability (Ehnvall, Ratcliffe, Bohlin, et al., 2023). This lag could result from initially unsuitable soil or climate conditions (Gorham et al., 2007; Morris et al., 2018) or slow plant dispersion/productivity rates (Sundberg et al., 2006; Tiselius et al., 2019). Our observations and interpretations still hold true at the landscape level, even if single mires' ages are overestimated when derived from the elevation above sea level (Ehnvall, Ratcliffe, Bohlin, et al., 2023) since the primary mire formation can be assumed to dominate in the region (Huikari, 1956), and because we focus on the entire mire population rather than on individual mires. Mire ages derived from elevation have been confirmed based on ^{14}C dating of basal ages in mires at different elevations from the wider BBL area (Ehnvall, Ratcliffe, Bohlin, et al., 2023), providing additional support for our approach.

Finally, the chronosequence approach assumes similar climate and microclimate conditions over the Holocene. There is a potential variance in current microclimate along the coastal-inland gradient in the SMC, but when compared to the wider boreal region, this variation is negligible (Yu et al., 2009). A lag in mire initiation, or halt in mire expansion, may happen under drier, less favorable conditions (Gorham et al., 2007; Morris

et al., 2018), while in contrast, episodic expansion patterns may appear under wetter, more favorable conditions (Korhola, 1996; Turunen & Turunen, 2003). Mires in the SMC experienced Holocene climate fluctuations typical of northern latitudes (Wastegård, 2022), with warm and dry conditions during the Holocene thermal maximum ~8,000–5,000 years BP, followed by a transition to colder and wetter conditions during the mid-Holocene (Loisel et al., 2014). During the 4,500–4,000 years BP period more variable climate conditions point towards a wet shift in many southern Swedish mires (Borgmark & Wastegård, 2008; de Jong et al., 2006). Around 2,800–2,600 years BP, the climate regime shifted from continental to oceanic in many parts of Sweden, i.e. more humid with less seasonal variation in temperature. This was followed by colder and drier conditions until ~1,500 years BP, after which the climate was wet and cold (Wastegård, 2022). Reports of a wet shift in mire hydrology (Rundgren et al., 2023) and increasing vertical peat accumulation rates (Larsson et al., 2017) have been reported from this period. Wetter and more suitable periods of Holocene climatic conditions may have enhanced the mire expansion patterns observed for the SMC. For example, the emergence of large mire complexes after ~2,000 years (Figures 2 and 4) coincides with the 2,800–2,600 years BP event and may partly reflect the rapid peat expansion to mire-suitable locations that were exposed from the sea during this wet shift in the Holocene climate. While climate variation should not be neglected, we maintain that the observed relationships between mire area, land-surface age, and topography support the idea that topography per se, rather than Holocene climate variation, is the main driver of present-day mire patterns in this region (Figure 5). As such, our research is ideally placed to answer questions related to topography and catchment water support. Nevertheless, there is still a clear gap in the literature that precludes making broad generalizations regarding the factors that drive mire development during glacial rebound. Indeed, the implications of our own findings could be much changed in a climate that supports both minerogenic and ombrogenic mires.

5. Conclusions

Patch size, arrangement, and spatial heterogeneity are important for a broad range of ecological, biogeochemical, and hydrological processes within individual mires—and for the dynamics of the boreal landscape mosaic as a whole. Our results reveal how spatial complexity can emerge during post-glacial succession. Further, we show that different spatial attributes of mires can reflect distinct drivers; for example, overall cover and shape complexity were linked to the formation of mire complexes over time, whereas mire abundance and fragmentation were driven by localized topographic controls. Such patterns can also manifest in complex ways as landscape age; while the youngest parts of the chronosequence supported predominantly small mires, older parts were characterized by a heterogeneous mix of small mires and large mire-complexes, reflecting a greater diversity of initiation and expansion pathways over time. Finally, our results underscore the influence of the surrounding upland topography and hydrology as a driver of mire size, shape, and arrangement across the northern boreal landscape.

Conflict of Interest

The authors declare no conflicts of interest relevant to this study.

Data Availability Statement

Data used in this study are available from the Swedish University of Agricultural Sciences Archive: https://hdl.handle.net/20.500.12703/4025 (Ehnvall, Ratcliffe, Nilsson, et al., 2023).

Acknowledgments
This work was funded by the Swedish Research Council Formas (Grants [2016-00896] and [2020-01436]) with supplementary support from the Swedish Nuclear Fuel and Waste Management Company.

References

Ågren, A. M., Hasselquist, E. M., Stendahl, J., Nilsson, M. B., & Paul, S. S. (2022). Delineating the distribution of mineral and peat soils at the landscape scale in northern boreal regions. *EGUsphere*, 1–23. https://doi.org/10.5194/egusphere-2022-79

Ågren, A. M., Larson, J., Paul, S. S., Laudon, H., & Lidberg, W. (2021). Use of multiple LIDAR-derived digital terrain indices and machine learning for high-resolution national-scale soil moisture mapping of the Swedish forest landscape. *Geoderma*, *404*, 115280. https://doi.org/10.1016/j.geoderma.2021.115280

Almquist-Jacobson, H., & Foster, D. R. (1995). Toward an integrated model for raised-bog development: Theory and field evidence. *Ecology*, *76*(8), 2503–2516. https://doi.org/10.2307/2265824

Arlen-Pouliot, Y., & Payette, S. (2015). The influence of climate on pool inception in boreal fens. *Botany*, *93*(10), 637–649. https://doi.org/10.1139/cjb-2015-0048

Autio, A., Ala-Aho, P., Ronkanen, A.-K., Rossi, P. M., & Kløve, B. (2020). Implications of peat soil conceptualization for groundwater exfiltration in numerical modeling: A study on a hypothetical peatland hillslope. *Water Resources Research*, *56*(8), e2019WR026203. https://doi.org/10.1029/2019WR026203

Borgmark, A., & Wastegård, S. (2008). Regional and local patterns of peat humification in three raised peat bogs in Värmland, south-central Sweden. *GFF*, *130*(3), 161–176. https://doi.org/10.1080/11035890809453231

Bring, A., Thorslund, J., Rosén, L., Tonderski, K., Åberg, C., Envall, I., & Laudon, H. (2022). Effects on groundwater storage of restoring, constructing or draining wetlands in temperate and boreal climates: A systematic review. *Environmental Evidence*, *11*(1), 38. https://doi.org/10.1186/s13750-022-00289-5

Cael, B. B., & Seekell, D. A. (2016). The size-distribution of Earth's lakes. *Scientific Reports*, *6*(1), 29633. https://doi.org/10.1038/srep29633

Chico, G., Clutterbuck, B., Lindsay, R., Midgley, N. G., & Labadz, J. (2019). Identification and classification of unmapped blanket bogs in the Cordillera Cantábrica, northern Spain. *Mires & Peat*, *24*. Art. 2. https://doi.org/10.19189/MaP.2018.AJB.378

Clark, P. U., Dyke, A. S., Shakun, J. D., Carlson, A. E., Clark, J., Wohlfarth, B., et al. (2009). The last glacial maximum. *Science*, *325*(5941), 710–714. https://doi.org/10.1126/science.1172873

Cohen, M. J., Creed, I. F., Alexander, L., Basu, N. B., Calhoun, A. J. K., Craft, C., et al. (2016). Do geographically isolated wetlands influence landscape functions? *Proceedings of the National Academy of Sciences of the United States of America*, *113*(8), 1978–1986. https://doi.org/10.1073/pnas.1512650113

Crawford, R. M. M., Jeffree, C. E., & Rees, W. G. (2003). Paludification and forest retreat in northern oceanic environments. *Annals of Botany*, *91*(2), 213–226. https://doi.org/10.1093/aob/mcf185

Damman, A. W. H. (1986). Hydrology, development, and biogeochemistry of ombrogenous peat bogs with special reference to nutrient relocation in a western Newfoundland bog. *Canadian Journal of Botany*, *64*(2), 384–394. https://doi.org/10.1139/b86-055

de Jong, R., Björck, S., Björkman, L., & Clemmensen, L. B. (2006). Storminess variation during the last 6500 years as reconstructed from an ombrotrophic peat bog in Halland, southwest Sweden. *Journal of Quaternary Science*, *21*(8), 905–919. https://doi.org/10.1002/jqs.1011

Ehnvall, B. (2023). Catchment controls on mire properties in the post-glacial landscape (Doctoral thesis). *Acta Universitatis Agriculturae Sueciae*, 73. https://doi.org/10.54612/a.2hq3ebpddu

Ehnvall, B., Ågren, A. M., Nilsson, M. B., Ratcliffe, J. L., Noumonvi, K. D., Peichl, M., et al. (2023). Catchment characteristics control boreal mire nutrient regime and vegetation patterns over ~5000 years of landscape development. *Science of the Total Environment*, *165132*, 165132. https://doi.org/10.1016/j.scitotenv.2023.165132

Ehnvall, B., Ratcliffe, J. L., Bohlin, E., Nilsson, M. B., Öquist, M. G., Sponseller, R. A., & Grabs, T. (2023). Landscape constraints on mire lateral expansion. *Quaternary Science Reviews*, *302*, 107961. https://doi.org/10.1016/j.quascirev.2023.107961

Ehnvall, B., Ratcliffe, J. L., Nilsson, M. B., Öquist, M. G., Sponseller, R., & Grabs, T. (2023). Size and shape in mires, as well as slope and moisture in mires and their surrounding upslope areas across 9000 years of mire development in the post-glacial landscape of the Sävar Rising Coastline Mire Chronosequence [Dataset]. Swedish University of Agricultural Sciences Archive. https://hdl.handle.net/20.500.12703/4025

Englund, G., Eriksson, H., & Nilsson, M. B. (2013). The birth and death of lakes on young landscapes. *Geophysical Research Letters*, *40*(7), 1340–1344. https://doi.org/10.1002/grl.50281

Fergus, C. E., Lapierre, J.-F., Oliver, S. K., Skaff, N. K., Cheruvelil, K. S., Webster, K., et al. (2017). The freshwater landscape: Lake, wetland, and stream abundance and connectivity at macroscales. *Ecosphere*, *8*, e01911. https://doi.org/10.1002/ecs2.1911

Forman, R. T. T., & Gordon, M. (1986). *Landscape ecology*. John Wiley & Sons.

Foster, D. R., & Glaser, P. H. (1986). The raised bogs of south-eastern Labrador, Canada: Classification, distribution, vegetation and recent dynamics. *Journal of Ecology*, *74*(1), 47–71. https://doi.org/10.2307/2260348

Fraixedas, S., Lindén, A., Meller, K., Lindström, Å., Keišs, O., Kålås, J. A., et al. (2017). Substantial decline of Northern European peatland bird populations: Consequences of drainage. *Biological Conservation*, *214*, 223–232. https://doi.org/10.1016/j.biocon.2017.08.025

Frolking, S., & Roulet, N. T. (2007). Holocene radiative forcing impact of northern peatland carbon accumulation and methane emissions. *Global Change Biology*, *13*(5), 1079–1088. https://doi.org/10.1111/j.1365-2486.2007.01339.x

Gałka, M., Tobolski, K., Lamentowicz, Ł., Ersek, V., Jassey, V. E. J., van der Knaap, W. O., & Lamentowicz, M. (2017). Unveiling exceptional Baltic bog ecohydrology, autogenic succession and climate change during the last 2000 years in CE Europe using replicate cores, multi-proxy data and functional traits of testate amoebae. *Quaternary Science Reviews*, *156*, 90–106. https://doi.org/10.1016/j.quascirev.2016.11.034

Gallego-Sala, A., & Prentice, I. C. (2013). Blanket peat biome endangered by climate change. *Nature Climate Change*, *3*(2), 152–155. https://doi.org/10.1038/NCLIMATE1672

Gardner, J. R., Pavelsky, T. M., & Doyle, M. W. (2019). The abundance, size, and spacing of lakes and reservoirs connected to river networks. *Geophysical Research Letters*, *46*(5), 2592–2601. https://doi.org/10.1029/2018GL080841

Gear, A. J., & Huntley, B. (1991). Rapid changes in the range limits of scots pine 4000 years ago. *Science*, *251*(4993), 544–547. https://doi.org/10.1126/science.251.4993.544

Glaser, P. H., Hansen, B. C., Siegel, D. I., Reeve, A. S., & Morin, P. J. (2004). Rates, pathways and drivers for peatland development in the Hudson Bay Lowlands, northern Ontario, Canada. *Journal of Ecology*, *92*(6), 1036–1053. https://doi.org/10.1111/j.0022-0477.2004.00931.x

Glaser, P. H., Siegel, D. I., Reeve, A. S., Janssens, J. A., & Janecky, D. R. (2004). Tectonic drivers for vegetation patterning and landscape evolution in the Albany River region of the Hudson Bay Lowlands. *Journal of Ecology*, *92*(6), 1054–1070. https://doi.org/10.1111/j.0022-0477.2004.00930.x

Glatzel, S., Worrall, F., Boothroyd, I. M., & Heckman, K. (2023). Comparison of the transformation of organic matter flux through a raised bog and a blanket bog. *Biogeochemistry*. https://doi.org/10.1007/s10533-023-01093-0

Gorham, E. (1957). The development of peat lands. *The Quarterly Review of Biology*, *32*(2), 145–166. https://doi.org/10.1086/401755

Gorham, E., Lehman, C., Dyke, A., Janssens, J., & Dyke, L. (2007). Temporal and spatial aspects of peatland initiation following deglaciation in North America. *Quaternary Science Reviews*, *26*(3–4), 300e311. https://doi.org/10.1016/j.quascirev.2006.08.008

Graniero, P. A., & Price, J. S. (1999). The importance of topographic factors on the distribution of bog and heath in a Newfoundland blanket bog complex. *Catena*, *36*(3), 233–254. https://doi.org/10.1016/S0341-8162(99)00008-9

Granlund, E. (1932). *De svenska högmossarnas geologi: deras bildningsbetingelser, utvecklingshistoria och utbredning jämte sambandet mellan högmossebildning och försumpning*. Sveriegs geologiska undersökning.

Gunnarsson, U., Löfroth, M., & Sandring, S. (2014). *The Swedish wetland survey: Compiled excerpts from the national final report*. Rapport/Naturvårdsverket. Swedish Environmental Protection Agency.

Hare, D. K., Boutt, D. F., Clement, W. P., Hatch, C. E., Davenport, G., & Hackman, A. (2017). Hydrogeological controls on spatial patterns of groundwater discharge in peatlands. *Hydrology and Earth System Sciences*, *21*(12), 6031–6048. https://doi.org/10.5194/hess-21-6031-2017

Helbig, M., Waddington, J. M., Alekseychik, P., Amiro, B., Aurela, M., Barr, A. G., et al. (2020a). The biophysical climate mitigation potential of boreal peatlands during the growing season. *Environmental Research Letters*, *15*(10), 104004. https://doi.org/10.1088/1748-9326/abab34

Helbig, M., Waddington, J. M., Alekseychik, P., Amiro, B. D., Aurela, M., Barr, A. G., et al. (2020b). Increasing contribution of peatlands to boreal evapotranspiration in a warming climate. *Nature Climate Change*, *10*(6), 555–560. https://doi.org/10.1038/s41558-020-0763-7

Hokanson, K. J., Peterson, E. S., Devito, K. J., & Mendoza, C. A. (2020). Forestland-peatland hydrologic connectivity in water-limited environments: Hydraulic gradients often oppose topography. *Environmental Research Letters*, *15*(3), 034021. https://doi.org/10.1088/1748-9326/ab699a

Howie, S. A., & Meerveld, I. T. (2011). The essential role of the lagg in raised bog function and restoration: A review. *Wetlands*, *31*(3), 613–622. https://doi.org/10.1007/s13157-011-0168-5

Huikari, O. (1956). Primäärisen soistumisen osuudesta Suomen soiden synnyssä. *Communicationes Instituti Forestalls Fenniae*, *46*, 1–79.

Ireland, A. W., & Booth, R. K. (2011). Hydroclimatic variability drives episodic expansion of a floating peat mat in a North American kettlehole basin. *Ecology*, *92*(1), 11–18. https://doi.org/10.1890/10-0770.1

Ireland, A. W., Booth, R. K., Hotchkiss, S. C., & Schmitz, J. E. (2013). A comparative study of within-basin and regional peatland development: Implications for peatland carbon dynamics. *Quaternary Science Reviews*, *61*, 85–95. https://doi.org/10.1016/j.quascirev.2012.10.035

Ivanov, K. (1981). *Water movement in mirelands*. Academic Press Inc.

Jaros, A., Rossi, P. M., Ronkanen, A.-K., & Kløve, B. (2019). Parameterisation of an integrated groundwater-surface water model for hydrological analysis of boreal aapa mire wetlands. *Journal of Hydrology*, *575*, 175–191. https://doi.org/10.1016/j.jhydrol.2019.04.094

Joosten, H. (2003). Wise use of mires: Background and principles 239–250.

Ketcheson, S. J., Price, J. S., Carey, S. K., Petrone, R. M., Mendoza, C. A., & Devito, K. J. (2016). Constructing fen peatlands in post-mining oil sands landscapes: Challenges and opportunities from a hydrological perspective. *Earth-Science Reviews*, *161*, 130–139. https://doi.org/10.1016/j.earscirev.2016.08.007

Kleinen, T., Brovkin, V., & Schuldt, R. J. (2012). A dynamic model of wetland extent and peat accumulation: Results for the Holocene. *Biogeosciences*, *9*(1), 235–248. https://doi.org/10.5194/bg-9-235-2012

Kolari, T. H. M., Korpelainen, P., Kumpula, T., & Tahvanainen, T. (2021). Accelerated vegetation succession but no hydrological change in a boreal fen during 20 years of recent climate change. *Ecology and Evolution*, *11*(12), 7602–7621. https://doi.org/10.1002/ece3.7592

Korhola, A. (1996). Initiation of a sloping mire complex in southwestern Finland: Autogenic versus allogenic controls. *Écoscience*, *3*(2), 216–222. https://doi.org/10.1080/11956860.1996.11682334

Korhola, A. A. (1994). Radiocarbon evidence for rates of lateral expansion in raised mires in southern Finland. *Quaternary Research*, *42*(3), 299–307. https://doi.org/10.1006/qres.1994.1080

Krachler, R., Krachler, R. F., Wallner, G., Steier, P., Abiead, Y. E., Wiesinger, H., et al. (2016). Sphagnum-dominated bog systems are highly effective yet variable sources of bio-available iron to marine waters. *Science of the Total Environment*, *10*.

Kulczyński, S. (1949). *Peat bogs of Polesie*. Academie Polonaise des Sciences et des Lettres.

Kutenkov, S. A., Kozhin, M. N., Golovina, E. O., Kopeina, E. I., & Stoikina, N. V. (2018). Polygonal patterned peatlands of the White Sea islands. *IOP Conference Series: Earth and Environmental Science*, *138*, 012010. https://doi.org/10.1088/1755-1315/138/1/012010

Laitinen, J., Rehell, S., & Oksanen, J. (2008). Community and species responses to water level fluctuations with reference to soil layers in different habitats of mid-boreal mire complexes. *Plant Ecology*, *194*(1), 17–36. https://doi.org/10.1007/s11258-007-9271-3

Lambert, C., Larocque, M., Gagné, S., & Garneau, M. (2022). Aquifer-peatland hydrological connectivity and controlling factors in boreal peatlands. *Frontiers in Earth Science*, *10*. https://doi.org/10.3389/feart.2022.835817

Lane, L., Autrey, L., Alexander, L. C., & LeDuc, S. D. (2018). Hydrological, physical, and chemical functions and connectivity of non-floodplain wetlands to downstream waters: A review. *Journal of the American Water Resources Association (JAWRA)*, *54*(2), 346–371. https://doi.org/10.1111/1752-1688.12633

Larsson, A., Segerström, U., Laudon, H., & Nilsson, M. B. (2017). Holocene carbon and nitrogen accumulation rates in a boreal oligotrophic fen. *The Holocene*, *27*, 811–821. https://doi.org/10.1177/0959683616675936

Lidberg, W., Nilsson, M., Lundmark, T., & Ågren, A. M. (2017). Evaluating preprocessing methods of digital elevation models for hydrological modelling. *Hydrological Processes*, *31*(26), 4660–4668. https://doi.org/10.1002/hyp.11385

Limpens, J., Holmgren, M., Jacobs, C. M., Van der Zee, S. E., Karofeld, E., & Berendse, F. (2014). How does tree density affect water loss of peatlands? A mesocosm experiment. *PLoS One*, *9*(3), e91748. https://doi.org/10.1371/journal.pone.0091748

Linden, M., Möller, P., Björck, S., & Sandgren, P. (2006). Holocene shore displacement and deglaciation chronology in Norrbotten, Sweden. *Boreas*, *35*(1), 1e22. https://doi.org/10.1080/03009480500359160

Lindsay, J. B. (2016). The practice of DEM stream burning revisited: The practice of DEM stream burning revisited. *Earth Surface Processes and Landforms*, *41*(5), 658–668. https://doi.org/10.1002/esp.3888

Liu, Y., Wagener, T., Beck, H. E., & Hartmann, A. (2020). What is the hydrologically effective area of a catchment? *Environmental Research Letters*, *15*(10), 104024. https://doi.org/10.1088/1748-9326/aba7e5

Loisel, J., Yu, Z., Beilman, D. W., Camill, P., Alm, J., Amesbury, M. J., et al. (2014). A database and synthesis of northern peatland soil properties and Holocene carbon and nitrogen accumulation. *The Holocene*, *24*(9), 1028–1042. https://doi.org/10.1177/0959683614538073

Loisel, J., Yu, Z., Parsekian, A., Nolan, J., & Slater, L. (2013). Quantifying landscape morphology influence on peatland lateral expansion using ground-penetrating radar (GPR) and peat core analysis. *Journal of Geophysical Research: Biogeosciences*, *118*(2), 373–384. https://doi.org/10.1002/jgrg.20029

Luoto, M., & Seppälä, M. (2000). Summit peats ('peat cakes') on the fells of Finnish Lapland: Continental fragments of blanket mires? *The Holocene*, *10*(2), 229–241. https://doi.org/10.1191/095968300670047420

Marttila, H., Aurela, M., Büngener, L., Rossi, P. M., Lohila, A., Postila, H., et al. (2021). Quantifying groundwater fluxes from an aapa mire to a riverside esker formation. *Hydrology Research*, *52*(2), 585–596. https://doi.org/10.2166/nh.2021.064

Moar, N. T. (1956). Peat on the Mokai Patea, Ruahine Range, North Island, New Zealand. *New Zealand Journal of Science and Technology*, 419–426.

Moore, P. A., Didemus, B. D., Furukawa, A. K., & Waddington, J. M. (2021). Peat depth as a control on Sphagnum moisture stress during seasonal drought. *Hydrological Processes*, *35*(4), e14117. https://doi.org/10.1002/hyp.14117

Morris, P. J., Swindles, G. T., Valdes, P. J., Ivanovic, R. F., Gregoire, L. J., Smith, M. W., et al. (2018). Global peatland initiation driven by regionally asynchronous warming. *Proceedings of the National Academy of Sciences of the United States of America*, *115*(19), 4851e4856. https://doi.org/10.1073/pnas.1717838115

Nilsson, M., Sagerfors, J., Buffam, I., Laudon, H., Eriksson, T., Grelle, A., et al. (2008). Contemporary carbon accumulation in a boreal oligotrophic minerogenic mire—A significant sink after accounting for all C-fluxes. *Global Change Biology*, *14*(10), 2317–2332. https://doi.org/10.1111/j.1365-2486.2008.01654.x

Nordman, M., Peltola, A., Bilker-Koivula, M., & Lahtinen, S. (2020). Past and future sea level changes and land uplift in the Baltic Sea seen by geodetic observations. In *International association of geodesy symposia*. Springer Berlin Heidelberg. https://doi.org/10.1007/1345_2020_124

Nordström, E., Eckstein, R. L., & Lind, L. (2022). Edge effects on decomposition in Sphagnum bogs: Implications for carbon storage. *Ecosphere*, *13*(9), e4234. https://doi.org/10.1002/ecs2.4234

Norstedt, G., Hasselquist, E., & Laudon, H. (2021). From haymaking to wood production: Past use of mires in northern Sweden affect current ecosystem services and function. *Rural Landscapes: Society, Environment, History*, *8*(1). https://doi.org/10.16993/rl.70

Novenko, E. Y., Tsyganov, A. N., Pisarchuk, N. M., Volkova, E. M., Babeshko, K. V., Kozlov, D. N., et al. (2018). Forest history, peatland development and mid- to late Holocene environmental change in the southern taiga forest of central European Russia. *Quaternary Research*, *89*(1), 223–236. https://doi.org/10.1017/qua.2017.91

O'Callaghan, J. F., & Mark, D. M. (1984). The extraction of drainage networks from digital elevation data. *Computer Vision, Graphics, and Image Processing*, *28*(3), 323–344. https://doi.org/10.1016/S0734-189X(84)80011-0

Ohlson, M., Økland, R. H., Nordbakken, J.-F., & Dahlberg, B. (2001). Fatal interactions between Scots pine and Sphagnum mosses in bog ecosystems. *Oikos*, *94*(3), 425–432. https://doi.org/10.1034/j.1600-0706.2001.940305.x

Påsse, T., & Daniels, J. (2015). *Past shore-level and sea-level displacements*. Sveriges geologiska undersökning.

Pearsall, W. H. (1950). *Mountains and moorlands*. Collins, New Naturalist.

Pilgrim, D. H., Cordery, I., & Baron, B. C. (1982). Effects of catchment size on runoff relationships. *Journal of Hydrology*, *58*(3–4), 205–221. https://doi.org/10.1016/0022-1694(82)90035-X

Rana, P., & Tolvanen, A. (2021). Transferability of 34 red-listed peatland plant species models across boreal vegetation zone. *Ecological Indicators*, *129*, 107950. https://doi.org/10.1016/j.ecolind.2021.107950

Ratcliffe, J. L., Creevy, A., Andersen, R., Zarov, E., Gaffney, P. P. J., Taggart, M. A., et al. (2017). Ecological and environmental transition across the forested-to-open bog ecotone in a west Siberian peatland. *Science of the Total Environment*, *607–608*, 816–828. https://doi.org/10.1016/j.scitotenv.2017.06.276

R Core Team. (2020). *A language and environment for statistical computing*. R Foundation for Statistical Computing. Retrieved from https://www.r-project.org/

Rehell, S., Laitinen, J., Oksanen, J., & Siira, O.-P. (2019). Mire margin to expanse gradient in part relates to nutrients gradient: Evidence from successional mire basins, north Finland. *Mires & Peat*, 1–12. https://doi.org/10.19189/MaP.2018.OMB.353

Renberg, I., & Segerström, U. (1981). The initial points on a shoreline displacement curve for southern Västerbotten, dated by varve-counts of lake sediments. *Striae*, *14*, 174–176.

Romanov, V. V. (1968). *Hydrographics of bogs*. Israel Programme for Scientific Translation.

Rundgren, M., Kokfelt, U., Schoning, K., & Wastegård, S. (2023). Holocene wet shifts in NW European bogs: Evidence for the roles of external forcing and internal feedback from a high-resolution study of peat properties, plant macrofossils and testate amoebae. *Journal of Quaternary Science*, *38*(3), 423–439. https://doi.org/10.1002/jqs.3485

Ruppel, M., Väliranta, M., Virtanen, T., & Korhola, A. (2013). Postglacial spatiotemporal peatland initiation and lateral expansion dynamics in North America and northern Europe. *The Holocene*, *23*(11), 1596–1606. https://doi.org/10.1177/0959683613499053

Rydin, H., Jeglum, J., & Bennett, K. (2013). *The biology of peatlands, 2e* (2nd ed.). Oxford University Press.

Rydin, H., Sjörs, H., & Löfroth, M. (1999). Mires. *Acta Phytogeographica Suecica*, *84*, 91–112.

Sallinen, A., Akanegbu, J., Marttila, H., & Tahvanainen, T. (2023). Recent and future hydrological trends of aapa mires across the boreal climate gradient. *Journal of Hydrology*, *617*, 129022. https://doi.org/10.1016/j.jhydrol.2022.129022

Sallinen, A., Tuominen, S., Kumpula, T., & Tahvanainen, T. (2019). Undrained peatland areas disturbed by surrounding drainage: A large scale GIS analysis in Finland with a special focus on aapa mires.

Scheffer, M., Hirota, M., Holmgren, M., Van Nes, E. H., & Chapin, F. S. (2012). Thresholds for boreal biome transitions. *Proceedings of the National Academy of Sciences of the United States of America*, *109*(52), 21384–21389. https://doi.org/10.1073/pnas.1219844110

Seibert, J., Stendahl, J., & Sørensen, R. (2007). Topographical influences on soil properties in boreal forests. *Geoderma*, *141*(1–2), 139–148. https://doi.org/10.1016/j.geoderma.2007.05.013

Silva, A. C., Barbosa, M. S., Barral, U. M., Silva, B. P. C., Fernandes, J. S. C., Viana, A. J. S., et al. (2019). Organic matter composition and paleoclimatic changes in tropical mountain peatlands currently under grasslands and forest clusters. *Catena*, *180*, 69–82. https://doi.org/10.1016/j.catena.2019.04.017

Sirin, A., Köhler, S., & Bishop, K. (1998). Resolving flow pathways and geochemistry in a headwater forested wetland with multiple tracers 248.

Sjörs, H. (1990). Divergent successions in mires, a comparative study. *Aquilo—Series Botanica*, *28*, 67–77.

Sjörs, H., & Gunnarsson, U. (2002). Calcium and pH in north and central Swedish mire waters. *Journal of Ecology*, *90*(4), 650–657. https://doi.org/10.1046/j.1365-2745.2002.00701.x

Sjöström, J. K., Martínez Cortizas, A., Hansson, S. V., Silva Sánchez, N., Bindler, R., Rydberg, J., et al. (2020). Paleodust deposition and peat accumulation rates—Bog size matters. *Chemical Geology*, *554*, 119795. https://doi.org/10.1016/j.chemgeo.2020.119795

Sponseller, R. A., Blackburn, M., Nilsson, M. B., & Laudon, H. (2018). Headwater mires constitute a major source of nitrogen (N) to surface waters in the boreal landscape. *Ecosystems*, *21*(1), 31–44. https://doi.org/10.1007/s10021-017-0133-0

Starr, M., & Lindroos, A.-J. (2006). Changes in the rate of release of Ca and Mg and normative mineralogy due to weathering along a 5300-year chronosequence of boreal forest soils. *Geoderma*, *133*(3–4), 269–280. https://doi.org/10.1016/j.geoderma.2005.07.013

Stroeven, A. P., Hättestrand, C., Kleman, J., Heyman, J., Fabel, D., Fredin, O., et al. (2016). Deglaciation of Fennoscandia. *Quaternary Science Reviews, Special Issue: PAST Gateways (Palaeo-Arctic Spatial and Temporal Gateways)*, *147*, 91–121. https://doi.org/10.1016/j.quascirev.2015.09.016

Stum-Boivin, É. L., Magnan, G., Garneau, M., Fenton, N. J., Grondin, P., & Bergeron, Y. (2019). Spatiotemporal evolution of paludification associated with autogenic and allogenic factors in the black spruce–moss boreal forest of Québec, Canada. *Quaternary Research*, *91*(2), 650–664. https://doi.org/10.1017/qua.2018.101

Sundberg, S., Hansson, J., & Rydin, H. (2006). Colonization of Sphagnum on land uplift islands in the Baltic Sea: Time, area, distance and life history. *Journal of Biogeography*, *33*(8), 1479e1491. https://doi.org/10.1111/j.1365-2699.2006.01520

Tiselius, A. K., Lundback, S., Lönnell, N., Jansson, R., & Dynesius, M. (2019). Bryophyte community assembly on young land uplift islands e dispersal and habitat filtering assessed using species traits. *Journal of Biogeography*, *46*, 2188e2202. https://doi.org/10.1111/jbi.13652

Treat, C. C., Jones, M. C., Alder, J., & Frolking, S. (2022). Hydrologic controls on peat permafrost and carbon processes: New insights from past and future modeling. *Frontiers in Environmental Science*, *10*. https://doi.org/10.3389/fenvs.2022.892925

Treat, C. C., Kleinen, T., Broothaerts, N., Dalton, A. S., Dommain, R., Douglas, T. A., et al. (2019). Widespread global peatland establishment and persistence over the last 130,000 y. *Proceedings of the National Academy of Sciences of the United States of America*, *116*(11), 4822–4827. https://doi.org/10.1073/pnas.1813305116

Turunen, C., & Turunen, J. (2003). Development history and carbon accumulation of a slope bog in oceanic British Columbia, Canada. *The Holocene*, *13*(2), 225e238. https://doi.org/10.1191/0959683603hl609rp

van der Velde, Y., Temme, A. J. A. M., Nijp, J. J., Braakhekke, M. C., van Voorn, G. A. K., Dekker, S. C., et al. (2021). Emerging forest–peatland bistability and resilience of European peatland carbon stores. *Proceedings of the National Academy of Sciences of the United States of America*, *118*(38). https://doi.org/10.1073/pnas.2101742118

van Breemen, N. (1995). How Sphagnum bogs down other plants. *Trends in Ecology & Evolution*, *10*(7), 270–275. https://doi.org/10.1016/0169-5347(95)90007-1

Wastegård, S. (2022). The Holocene of Sweden—A review. *GFF*, *144*(2), 126–149. https://doi.org/10.1080/11035897.2022.2086290

Weckström, J., Seppä, H., & Korhola, A. (2010). Climatic influence on peatland formation and lateral expansion in sub-Arctic Fennoscandia. *Boreas*, *39*(4), 761–769. https://doi.org/10.1111/j.1502-3885.2010.00168.x

White, M., & Payette, S. (2016). Pool size structure indicates developmental stages of boreal fens. *Botany*, *94*(8), 643–651. https://doi.org/10.1139/cjb-2015-0268

Winter, T. C. (1988). A conceptual framework for assessing cumulative impacts on the hydrology of nontidal wetlands. *Environmental Management*, *12*(5), 605–620. https://doi.org/10.1007/BF01867539

Yu, Z., Beilman, D. W., & Jones, M. C. (2009). Sensitivity of northern peatland carbon dynamics to Holocene climate change. *Carbon Cycling in Northern Peatlands*, *184*, 55–69. https://doi.org/10.1029/2008GM000822

Zevenbergen, L. W., & Thorne, C. R. (1987). Quantitative analysis of land surface topography. *Earth Surface Processes and Landforms*, *12*(1), 47–56. https://doi.org/10.1002/esp.3290120107